Characterization of Non-Volatile Oxidation Products Formed from Triolein in a Model Study at Frying Temperature

Sílvia Petronilho [a,b,*], Bruna Neves [c], Tânia Melo [c,d], Sara Oliveira [a], Eliana Alves [c], Cristina Barros [c], Fernando Nunes [b], Manuel A. Coimbra [a], M. Rosário Domingues [c,d]

[a] *LAQV-REQUIMTE, Department of Chemistry, University of Aveiro, Campus Universitário de Santiago, 3810-193, Aveiro, Portugal*

[b] *Chemistry Research Centre-Vila Real, Department of Chemistry, University of Trás-os-Montes and Alto Douro, Quinta de Prados, Vila Real, 5001-801, Portugal*

[c] *Mass Spectrometry Centre, LAQV-REQUIMTE, Department of Chemistry, University of Aveiro, Campus Universitário de Santiago, 3810-193 Aveiro, Portugal*

[d] *CESAM, Centre for Environmental and Marine Studies, Department of Chemistry, University of Aveiro, Campus Universitário de Santiago, 3810-193 Aveiro, Portugal*

* Corresponding author

E-mail address: silviapetronilho@ua.pt (S. Petronilho)

Abstract

Frying allows cooking food while promoting their organoleptic properties, imparting crunchiness and flavor. The drawback is the oxidation of triacylglycerides (TAGs), leading to the formation of primary oxidized TAGs. Although they have been associated with chronic and degenerative diseases, they are precursors of pleasant flavors to fried foods. Nevertheless, there is a lack of knowledge about the oxidation species present in foods and their involvement in the positive/negative health effects. In this work, high-resolution C_{30} reversed-phase (RP)-liquid chromatography (LC)-tandem high-resolution mass spectrometry (MS/MS) was used to identify primary oxidation TAGs resultant from heating triolein (160 ºC, 5 min). This allows simulating the initial heating process of frying oils usually used to prepare fried foods, as chips, crisps, and snacks. Beyond hydroxy, dihydroxy, hydroperoxy, and hydroxy-hydroperoxy derivatives, already reported in phospholipids Fenton oxidation, new compounds were identified, as dihydroxy-hydroperoxy-triolein derivatives and positional isomers (9/10- and 9/12-dihydroxy-triolein derivatives). These compounds should be considered when proposing flavor formation pathways and/or mitigating lipid-derived reactive oxygen species occurring during food frying.

Keywords: Frying oil; triacylglycerides; primary oxidation products; triolein; C_{30} RP-LC-MS; isomers differentiation.

Introduction

Frying is one of the most widely used method for cooking, allowing to produce fried foods in which taste, flavor, crunchiness, and texture are considered key quality parameters. The frying process involves heating the frying oil followed by dipping the raw materials within this oil, at high temperatures and in the presence of atmospheric oxygen, through simultaneous mass and heat transfer,[1, 2] allowing to cook the food while dehydrating and increasing their nutrient content. During this process, the characteristic fried food flavor is also formed, mainly due to the appearance of dienals, alkenals, lactones, hydrocarbons, and various cyclic compounds resultant from fatty acids oxidation,[3] including those resultant from triolein and trilinolein.[4] Moreover, the carbonyl compounds that are formed during foods frying can react with foods' amino acids, amines, and proteins, producing desirable and nutty pyrazines.[5]

Even though frying helps in the development of flavoring and color production via Maillard reaction,[6] it also leads to the occurrence of chemical alterations on the frying oil components,[7] and in processed foods, mainly in high-fat ones. Hydrolysis, oxidation, and/or polymerization of triacylglycerides (TAGs) have been reported.[3] These modifications affect cooking oils and foods' nutritional quality and cause the accumulation of off-flavors and undesirable compounds over the frying period, due to the repeated use of cooking oil, or even due to long-term storage.[8, 9] The antioxidants present in oils and foods influence the oils' quality during frying, decreasing their oxidation level.[3] However, beyond volatilization and/or decomposition phenomena, the effectiveness of the antioxidants against reactive oxygen species may decrease due to the lack of knowledge related to the multiple oxidation species that are formed during the frying process.

Lipid oxidation is a very complex process that leads to the formation of numerous products, mainly formed due to (poly)unsaturated fatty acids' oxidation by radical (e.g. thermal) oxidation,[6] that can be subsequently oxidized to secondary oxidation products, as aldehydes and carboxylates.[10, 11] In the case of frying oil, the higher extent of lipid oxidation reactions depends on several factors, as the amount of unsaturated fatty acids of the frying oil, temperature, atmospheric oxygen, and moisture.[12] Although precursors of the characteristic flavor of fried foods, the formation of these oxidized TAG products are also associated with the decrease of oils' quality, with consequent deleterious effects on food flavor, and is related to colon carcinogenesis.[13, 14]

Cooking oils oxidation can be deduced from the determination of the concentration of primary oxidation products in terms of the peroxide value (titration) and conjugated dienic systems, namely using ultraviolet–visible (UV-Vis) spectroscopy.[15, 16] However, the specific structure of primary lipid oxidation products needs to be determined by specific tools such as nuclear magnetic resonance (NMR),[10, 17-20] high-performance liquid chromatography (HPLC),[21-26] and gas chromatography.[27] Mass spectrometry (MS)-based approaches have also been used and considered promising for the analysis of TAG oxidation products,[9, 21, 28, 29] allowing their structural elucidation without sample derivatization or previous hydrolysis.

LC-electrospray ionization (ESI)-MS and LC-ESI-MS/MS have been used to identify hydroperoxy and epoxy TAGs.[9, 28, 29] Moreover, the C_{30} reversed-phase (RP)-LC-MS/MS approach using high-resolution (HR) MS platforms has already been successfully used to identify oxidation products of phospholipids, including the ones with oleic acid in their composition, as well as hydroxy-, dihydroxy-, and hydroxy-hydroperoxy-phospholipid derivatives.[30-32] Thus, it was hypothesized that high-throughput analytical methods, such as the C_{30} RP-LC-MS/MS, could allow to

deeply identify the TAG oxidation species, which should be considered when mitigating reactive oxygen species and/or flavor formation pathways occurring during the frying process. In this work, this strategy was used to simultaneously identify, structurally characterize, and differentiate isomers of primary oxidation TAGs, using triolein as a frying oil model, mimicking the initial conditions of heating the frying oils, preparing them for the contact with foods, contributing to understand which TAG oxidized species are involved when foods are fried.

Materials and Methods

Reagents and standards

Triolein (ref. Y0001113, purity ≥ 99.0%), used as frying oil TAG model, was obtained from Sigma-Aldrich (Darmstadt, Germany). The internal standard 1,3-ditetradecanoyl-2-(9*Z*-hexadecanoyl)-glycerol (MPoM - 14:0/16:1/14:0, ref.110558) was obtained from Avanti Polar Lipids, Inc. (Alabaster, AL, USA). All the organic solvents used had HPLC purity (99.9%) and were from Fisher Scientific Ltd. (Leicestershire, UK): chloroform, methanol (MeOH), acetonitrile, isopropanol. Ammonium formate and formic acid were from Sigma-Aldrich (St Louis, MO, USA). Ultra-pure water was used for all experiments, filtered through a 0.22-µm filter (Milli-Q Millipore system, Synergy®, Millipore Corporation, Billerica, MA, USA).

Triolein short-thermal treatment

Triolein was weighed (≈ 1.0 mg) in a test tube and submitted to thermal heating (160 ºC), in a block heater (Techne Dri - Block® DB-3A), for 5 minutes, and a surface-to-volume ratio of *ca*. 0.8 cm^{-1} was used. After cooling, approximately 1.0 mL of chloroform was added to triolein (final concentration of 1.0 mg mL^{-1}) and the samples

were immediately analyzed. A total of 3 independent replicates were made, each one corresponding to a different experiment.

C_{30} RP-LC-mass spectrometry (MS) and tandem MS (MS/MS)

Triolein primary oxidation products were analyzed by RP-LC-MS and MS/MS using a RP column with a C_{30} stationary phase. An UltiMate 3000™ UHPLC system (Thermo Fisher Scientific, Germering, Germany) was coupled online to a Q Exactive™ hybrid quadrupole-Orbitrap mass spectrometer (Thermo Fisher, Scientific, Bremen, Germany). The mobile phases consisted of water/acetonitrile (50:50, by volume) with 0.1% formic acid and 5 mM ammonium formate (phase A), and isopropanol/acetonitrile/water (85:10:5, by volume) with 0.1% formic acid and 5 mM ammonium formate (phase B). The solvent gradient started with 50% B held for 2 min followed by a linear increase to 86 % B in 18 min (at 20 min). An increase to 95 % B occurred in 1 min (at 21 min), which was isocratically held for 14 min (at 35 min), followed by a decrease to 50 % in 2 min (at 37 min), and maintained for 8 min until the end of the run (at 45 min). The flow rate was 300 µL min^{-1}.

The oxidized triolein (5 min, at 160 ºC, 1 mg mL^{-1}) and the internal standard MPoM (0.04 mg mL^{-1}), used for quality control purposes, were dissolved in chloroform. A volume of 5 µL of a mixture containing 20 µL (20 µg) of thermally treated triolein, 5 µL (200 ng) of MPoM, and 75 µL of MeOH were introduced into an Accucore™ C_{30} column (150 × 2.1 mm) equipped with 2.6 µm diameter fused-core particles (Thermo Fisher Scientific, Germering, Germany). The same procedure was performed for the non-treated triolein (1 mg mL^{-1}). For the full MS experiments, the Q Exactive™ HF hybrid quadrupole-Orbitrap mass spectrometer operated in positive-ion mode (electrospray voltage 3 kV) with a capillary temperature of 350 ºC; a sheath gas flow of 45 arbitrary

units (a.u.), an auxiliary gas flow of 15 a.u., a resolution of 70000, a maximum injection time of 100 ms, an AGC target of 1×10^6, and with a mass range between 400 and 1600 *m/z*. The tandem mass spectra of $[M+NH_4]^+$ precursor ions were obtained with a resolution of 17500, a maximum injection time of 100 ms, an automatic gain control (AGC) target of 1×10^5, and with an isolation window of 1 *m/z*. Cycles consisted of one full scan mass spectrum and ten data-dependent MS/MS scans that were repeated continuously throughout the experiments with a dynamic exclusion of 60 s, and an intensity threshold of 5×10^4. Normalized collision energy™ (NCE) was stepped between 20, 23, and 25 eV. Three injections (*n*=3) were performed respectively for the non and thermally treated triolein (160 ºC, 5 min), each one corresponding to the analysis of one different aliquot (*ca.* 1 mg of triolein). The orbitrap mass spectrometer was calibrated every week, according to the MS manufacturer instructions (calibrators included: Pierce LTQ Velos ISI Positive Ion calibration solution (ref. 88323) and Pierce ESI Negative Ion Calibration Solution (ref. 88324), from Fisher).

Data Analysis

Data acquisition was carried out using the Xcalibur data system (V3.3, Thermo Fisher Scientific, Waltham, MA, USA). The identification of oxidized triolein molecular species was based on the assignment of accurate mass measurements (error < 5 ppm) and the elemental composition of the precursor ions that were observed in the LC-MS spectra. The structural characterization of each oxidized TAG molecule was based on the MS/MS data by the identification of well-known fragmentation pattern of TAGs as $[M+NH_4]^+$ ions observed in the MS/MS spectra of each ion, as described in the literature,[33] as well as expected retention time (RT) and mass accuracy with an error of 5 ppm. The exact mass values were calculated using Scientific Instrument Services Exact Mass Calculator

(https://www.sisweb.com/referenc/tools/exactmass.htm) while the mass errors (≤ 5 ppm) were determined using the free web calculator available at https://warwick.ac.uk/fac/sci/chemistry/research/barrow/barrowgroup/calculators/mass_errors/.

Results

To evaluate the effect of frying temperatures in the cooking oils composition, triolein, a major monounsaturated TAG, found in vegetable and edible oils, composed by three oleic acid (OA) residues, was submitted to 160 ºC, for 5 min, simulating the common initial thermal frying process to heat the frying oils, preparing them to be in contact with foods, usually used for example for chips, crisps, and snacks. The thermally-oxidized products of this frying oil simulant were analyzed by high-resolution C_{30}-RP-LC-ESI-MS/MS. Full MS spectra acquired in positive-ion mode, before and after 5 min of thermal treatment at 160 ºC, are shown in Figure S1. In the C_{30}-LC-MS conditions used, the primary oxidation products of triolein were observed as $[M+NH_4]^+$ ions, and a total of 7 ions were assigned as triolein oxidation derivatives (Table 1). Initial structural identification and annotation of the oxidation products were based on accurate mass measurement against an in-house database (error < 5 ppm). Confirmation of the structural features of TAG oxidation products was achieved by the analysis of individual MS/MS spectra and interpretation of the characteristic MS/MS fragmentation pattern of each ion, thus enabling the assignment of several primary isomeric oxidation products (Table 1).

The ions attributed to TAG oxidation products were observed as $[M+NH_4]^+$ ions at *m/z* values higher than the non-modified triolein ($[M+NH_4]^+$ at *m/z* 902.818, Figure S1A), and identified at *m/z* 916.797, *m/z* 918.813, *m/z* 932.792, *m/z* 934.808, *m/z* 948.787,

175 *m/z* 950.802, and *m/z* 966.797, thus corresponding to mass shifts of +14 (O-2Da), +16
176 (O), +30 (2O-2Da), +32 (2O), +46 (3O-2Da), +48 (3O), and +64 (4O), respectively
177 (Figure S1B). These ions were assigned as hydroxy-, dihydroxy-, hydroperoxy-,
178 dihydroperoxy-, hydroxy-hydroperoxy-, dihydroxy-hydroperoxy-, epoxy-, epoxy-
179 hydroxy-, and epoxy-hydroperoxy-triolein derivatives, as summarized in Table 1.
180 However, the presence of keto-triolein derivatives (+ 14 Da) or even the epoxidation of
181 the double bonds (+ 16 Da) cannot be excluded since the methodology herein used was
182 not able to discriminate between epoxy and keto moieties.

183 The extracted ion current (XIC) chromatograms of triolein and of its main
184 oxidation products were plotted in Figure S2. The XIC chromatograms plotted for each
185 *m/z* of interest often resulted in more than one peak, thus allowing to discriminate between
186 structural and positional isomers that were further confirmed and identified by tandem
187 mass spectrometry (MS/MS). Under the C_{30}-LC conditions used, species with more
188 modifications eluted at shorter RTs, since the addition of functional groups containing
189 oxygen increased the polarity of the oxidized derivatives when compared with the non-
190 modified TAG (Table 1, Figure S2). The non-modified triolein was identified as
191 $[M+NH_4]^+$ ion, at *m/z* 902.818, which eluted at RT 26.99 min (Figure S2A). The MS/MS
192 spectrum showed a major product ion at *m/z* 603.533 formed due to the neutral loss (NL)
193 of OA chain (NL 282 Da) as an acid derivative (RCOOH), plus NH_3. The acylium (RCO^+)
194 and monoglyceride ions (RCO^+ + 74) of OA were also present at *m/z* 265.252 and
195 *m/z* 339.288, respectively (Figure S3).

196 Previous studies on TAG fragmentation under MS/MS conditions have reported
197 that the NL of the fatty acid linked to the *sn*-1 and *sn*-3 positions in the TAG glycerol
198 backbone is energetically favored in comparison with the NL of the fatty acid at *sn*-2
199 position, since at the *sn*-2 position there is a higher number of impediments, torsions, and

stresses.[34, 35] Thus, diacylglyceride (DAG) fragment ions formed due to the NL of the fatty acid at *sn*-2 should exist at lower relative abundance. Based on this and in the obtained results, it is possible to suggest the *sn*-2 position to be the less prone to be modified, thus retaining the non-modified fatty acyl chain. In the different constructed figures, this principle was used to represent the identified oxidized triolein derivatives. However, other possibilities for the positional isomers of the represented triolein derivatives cannot be excluded.

Hydroxy-triolein derivatives

The identified hydroxy derivatives (M+16) of triolein, at *m/z* 918.813, eluted in two peaks at RT 23.26 and 24.23 min (Figure S2B). The MS/MS spectrum of the ion eluting at RT 23.26 min (Figure 1A) showed the product ions at *m/z* 603.533 and *m/z* 619.523, formed by the NL of 298 Da and 282 Da, respectively, corresponding to the NL of the hydroxy OA and the non-modified OA as RCOOH, respectively, plus NH_3. However, based on the obtained MS/MS spectrum it was not possible to determine the position of the OH group on the OA chain. Moreover, in this spectrum, the most abundant product ion at *m/z* 601.518 was attributed to the combined NL of non-modified OA + NH_3 plus a NL of H_2O.

On the other hand, the MS/MS spectra of the ions that eluted as a major peak at RT 24.23 min (Figure 1B) revealed an abundant product ion at *m/z* 603.534, formed by the loss of 298 Da (corresponding to the NL of OA+16, as RCOOH) plus NH_3, which means the NL of the oxidized OA, and the ion at *m/z* 619.528, formed by the loss of 282 Da (corresponding to the NL of the non-modified OA) plus NH_3. Product ions at *m/z* 477.394 and *m/z* 493.387 were formed due to the fragmentation involving the cleavage of the OA chain in the vicinity of the carbon bearing the hydroxyl group. These

product ions allowed to pinpoint the position of the hydroxy (OH) group in C10 and C9, respectively (Figure S4). This allowed to propose the co-elution of the two positional isomers bearing the hydroxyl group in C10 and C9, respectively, similarly to what has been previously reported for hydroxy derivatives in aminophospholipids.[31]

Both MS/MS spectra (Figure 1A, B) showed the NL of H_2O (18 Da) at *m/z* 883.77 that was not present in the MS/MS spectrum of the non-modified triolein (Figure S3), thus corroborating the presence of the hydroxy derivative of triolein. However, the presence of a cyclic structure due to the epoxidation of the double bonds of two different oleic acid chains cannot be excluded since the methodology herein used was not able to discriminate between this kind of epoxy structure and hydroxy moieties.

Dihydroxy-triolein derivatives

The dihydroxy derivatives (M+32) of triolein, at *m/z* 934.808, eluted at RT 22.35 min and RT 22.52 min (Table 1 and Figure S2B). The MS/MS spectrum of the ions eluting at RT 22.35 min (Figure 1C) showed a major product ion at *m/z* 619.528, due to the NL of a hydroxy-OA (NL 298 Da, NL of OA+16). This indicates that this isomer of OA+2O corresponds to a dihydroxy derivative, and thus, each OH was present in different OA chains. The low relative abundance of fragment ions at *m/z* 603.531 (formed due to the combined loss of OA+2O plus loss of H_2O) confirms the insertion of two oxygen atoms in two different OA chains. Moreover, the NL of H_2O_2 (34 Da) was not found in this MS/MS spectrum (Figure 1C) being only observed the NL of H_2O (18 Da), thus corroborating the presence of a dihydroxy derivative of triolein. Moreover, the ions at *m/z* 477.392 plus *m/z* 507.404 and the ion at *m/z* 493.387 allowed pointing the position of the 2 hydroxy groups in C10 and C9, respectively, but in two OA chain moieties (Figure 1C). The product ion at *m/z* 509.382 can be formed due to the cleavage of one of

the OA chains between C9-C10, with the formation of a terminal aldehyde group in C9, also carrying a hydroxy moiety in C10 on the other OA chain.

Another TAG dihydroxy derivative from triolein + 2O, at *m/z* 934.808, eluting at RT 22.52 min (Table 1 and Figure 1D), bearing the two hydroxy moieties within the same OA chain, was determined according to the identification based on the MS/MS spectrum in Figure 1D. The abundant product ion at *m/z* 603.533, formed due to the NL of 314 Da (282 + 32), confirmed the insertion of two oxygen atoms in the same fatty acid. Once again, the NL of H_2O_2 was absent, while the NL of H_2O was found, thus corroborating the absence of a hydroperoxy moiety and the presence of hydroxy groups. The minor diagnostic product ions at *m/z* 479.372 and *m/z* 493.387 indicated the presence of the hydroxy groups in C8 and C9, respectively (Figure 1D).

Hydroperoxy-triolein derivatives

The oxidation product of triolein + 2O, at *m/z* 934.808, eluted in 3 peaks, one major peak at RT 23.12 min, and minor peaks at RT 22.35 min and 22.52 min (Table 1 and Figure S2B). The major peak was assigned as the hydroperoxy derivative based on the analysis of the tandem MS spectrum of the ion eluted at RT 23.12 min (Figure 2A). In this spectrum, it was observed the NL of 34 Da plus NH_3, with the formation of the ion at *m/z* 883.775, corresponding to the NL of H_2O_2 plus NH_3, which is typical of hydroperoxy derivatives.[31]

The product ion at *m/z* 603.533 was assigned to the combined loss of OA + 2O and the NL of NH_3, also corroborating the presence of a hydroperoxy derivative. The product ions at *m/z* 493.389, and at *m/z* 477.396 and *m/z* 507.404, formed due to the cleavage in the vicinity of the carbon linked to the hydroperoxy moiety, allowed to locate

274 the hydroperoxy group in C9 and C10, respectively, indicating the co-elution of two
275 positional isomers (Figure 2A). However, other positional isomers cannot be excluded.
276
277 **Dihydroperoxy-triolein derivatives**
278 In the case of $[M+NH_4]^+$ ions of triolein + 4O (*m/z* 966.797), the XIC
279 chromatogram showed a broader distribution, but only 3 major peaks at RT 18.09 min,
280 19.07 min, and 22.52 min were assigned as triolein oxidation products that were
281 characterized by MS/MS (Table 1 and Figure S2B). From these, the ones at 19.07 min
282 and 22.52 min were identified as dihydroperoxy derivatives of triolein.
283 The tandem MS spectrum of triolein + 4O, at RT 19.07 min (Figure 2B), showed
284 a highly abundant product ion at *m/z* 881.755, that may be formed by the combined loss
285 of two -OOH (2 x 34 Da), thus corroborating the presence of a dihydroperoxy derivative
286 of triolein. Furthermore, the presence of the fragment ion at *m/z* 601.517 indicates that
287 these two -OOH were placed in different OA chains. The hydroperoxy groups were
288 proposed to be located at C8 and C10 or C9 and C10 based on the identification of product
289 ions at *m/z* 479.371 (C8 position), *m/z* 493.388 (C9 position), and *m/z* 507.405 (C10
290 position).
291 The LC-MS/MS spectrum of triolein + 4O at RT 22.52 min (Figure 2C) showed
292 a highly abundant fragment ion of the non-modified DAG ion at *m/z* 603.533, formed due
293 to the NL of 346 Da (NL of OA + 4O) plus NH_3, corresponding the presence of 4 oxygens
294 in the same OA chain, while the NL of non-modified OA combined with NH_3, was seen
295 at *m/z* 667.508. The higher relative abundance of the ions at *m/z* 603.533 corroborated the
296 presence of a modified derivative in one fatty acyl chain plus NH_3, proposed as a
297 dihydroperoxy derivative, confirming the presence of the 4 oxygen atoms in the same OA
298 chain. This MS/MS spectrum showed the presence of minor diagnostic ions at *m/z*

493.390, and *m/z* 509.382 and *m/z* 465.356, which allowed proposing the modifications at C9/C12 and C7/C10, respectively (Figure 2C). Other isomers' possibilities cannot be excluded.

Hydroxy-hydroperoxy-triolein derivatives

The $[M+NH_4]^+$ ions of triolein + 3O (*m/z* 950.802) eluted in two chromatographic peaks at RT 20.86 and 22.45 min (Table 1 and Figure S2B). The LC-MS/MS spectrum of triolein + 3O at RT 20.86 min (Figure 3A) showed the ions at *m/z* 899.765 (NL of 34 Da, corresponding to the NL of H_2O_2, plus NH_3), *m/z* 881.755 (NL of 52 Da, combined NL of H_2O_2 plus H_2O, plus NH_3), and *m/z* 619.527 (NL of 314 Da, corresponding to the NL of 282 + 2O, plus NH_3), corroborating the presence of a hydroxy-hydroperoxy derivative, with the OOH moiety in one OA chain and the OH in another OA. The lower relative abundance of the ion at *m/z* 603.533 (NL of 330 Da, assigned to the NL of 282 + 48 Da plus NH_3), which corresponds to the non-modified DAG ion, and the presence of the ion at *m/z* 601.517 (NL of H_2O from ions at *m/z* 619.527) corroborate that the modifications occur in different OA chains.

Otherwise, the LC-MS/MS spectrum of triolein + 3O at RT 22.45 min (Figure 3B) showed an opposite trend since the ion at *m/z* 603.533 (NL of 330 Da, assigned to the NL of 282 + 48 Da plus NH_3) was the major fragment ion, thus proposing that both hydroxy and hydroperoxy moieties were present in the same fatty acyl chain. Furthermore, the MS/MS spectra revealed minor diagnostic product ions at *m/z* 493.387 and *m/z* 507.369, and *m/z* 477.396, that indicated the positions of the hydroxyl and the hydroperoxyl groups in C9 and C10, respectively (Figures 3A), and at *m/z* 493.388 pinpointing the position of the hydroxyl group in C9 (Figure 3B). However, other positional isomers cannot be excluded.

Dihydroxy-hydroperoxy-triolein derivatives

Based on the XIC chromatogram of $[M+NH_4]^+$ ions of triolein + 4O, at *m/z* 966.797 (Table 1 and Figure S2B), a peak eluting at RT 18.09 min can be identified as a dihydroxy-hydroperoxy derivative of triolein. As can be seen in Figure 3C, the LC-MS/MS spectrum of the triolein + 4O showed the NL of 348 Da, at *m/z* 601.517, corresponding to the combined NL of OA + 3O (-330 Da) plus the loss of H_2O (-18 Da) and the loss of NH_3. Moreover, the neutral loss of hydroxy-OA plus NH_3 plus the NL of H_2O, at *m/z* 633.505, the NL of hydroxy-OA (NL of 298 Da), at *m/z* 651.516, and the NL of OA + 2O (-314 Da) plus NH_3 plus the NL of H_2O (-18 Da), at *m/z* 617.510 were also observed. This indicated the presence of an isomer with a TAG esterified with one OA bearing three oxygens, thus a hydroxy-hydroperoxy-OA and a hydroxy-OA and a non-modified OA.

The presence of diagnostic ions at *m/z* 479.373, *m/z* 493.390, and *m/z* 507.367 allowed to pinpoint the position of the modified groups in C8 and C9, respectively, in different OA chains (Figure 3C). Other isomers' possibilities cannot be excluded.

Epoxy-triolein derivatives

The epoxy derivative (M+14) of triolein, at *m/z* 916.797, eluted in two peaks at 23.46 and 23.86 min (Table 1 and Figure S2B). The MS/MS spectrum of the ion eluting at RT 23.46 min (Figure 4A) showed abundant product ions at *m/z* 603.533 and *m/z* 617.511, formed due to the NL of 296 Da and 282 Da, corresponding to the NL of the epoxy OA and the non-modified OA as RCOOH, respectively, plus NH_3. In this spectrum, the most abundant product ion, at *m/z* 599.501, was attributed to the combined neutral loss of non-modified OA+NH_3 with the NL of H_2O.

The MS/MS spectrum of the ions that eluted at a major peak at 23.86 min (Figure 4B) showed an abundant product ion at *m/z* 603.533, formed by the loss of 296 Da (corresponding to the NL of OA+14 as RCOOH) plus NH_3, which means the NL of the oxidized OA, and the ion at *m/z* 617.513, formed by the loss of 282 Da (corresponding to the NL of the non-modified OA) plus NH_3. Other product ions at *m/z* 507.404, *m/z* 493.387, and *m/z* 479.374 were also observed and they were formed due to the fragmentation involving the cleavage of the oleic fatty acyl chain in the vicinity of the carbon bearing the hydroxy group. These product ions allowed to pinpoint the position of the epoxy (>O) group in C10, C9, and C8, respectively, and allowed to propose the co-elution of the three positional isomers bearing the epoxy group in C10, C9 and C8, respectively (Figure 4B). However, the presence of a keto-triolein derivative cannot be excluded since the methodology herein used was not able to discriminate between the keto and epoxy moieties.

Epoxy-hydroperoxy-triolein derivatives

The epoxy-hydroperoxy derivative (M+46 Da) of triolein, at *m/z* 948.787, eluted in two peaks, at RT 19.58 min and 22.65 min (Table 1 and Figure S2B). The MS/MS spectra of the ions eluting at these retention times (Figure 4C, D), revealed abundant product ions at *m/z* 617.511 and *m/z* 603.533, respectively, corresponding to the NL of the hydroperoxy OA, formed due to the NL of 314 Da, and the NL of an OA carrying both epoxy and hydroperoxyl groups, formed due to the NL of 328 Da, respectively, plus NH_3. This indicated the presence of an isomer with a TAG esterified with one OA bearing 2 oxygens and the other in another OA chain, as well as another isomer with a TAG esterified with one OA bearing all the 3 oxygens, thus carrying both >O and OOH groups. Moreover, a minor product ion at *m/z* 493.389 was also observed in both MS/MS spectra,

and it was formed due to the fragmentation involving the cleavage of the oleic fatty acyl chain in the vicinity of the carbon bearing the hydroperoxyl group. This allowed pinpointing the position of the OOH group in the C9 in both isomers (Figure 4C, D). However, other positional isomers cannot be excluded.

Epoxy-hydroxy-triolein derivatives

The epoxy-hydroxy derivative (M+30 Da) of triolein, at *m/z* 932.792, eluted in three peaks at RT 21.49 min, RT 22.25 min, and RT 23.05 min (Table 1 and Figure S2B). The MS/MS spectrum of the ion eluting at RT 21.49 min (Figure 5A) showed abundant product ions at *m/z* 633.506, *m/z* 615.496, *m/z* 603.533, and *m/z* 617.512, formed due to the NL of 282 Da, 300 Da, 312 Da, and 298 Da, corresponding to the NL of the non-modified OA as RCOOH, the epoxy OA, the epoxy-hydroxy OA, and the hydroxy OA, respectively, plus NH_3. Also, in this MS/MS spectrum, the minor product ion at *m/z* 493.388 allowed to pinpoint the position of the OH group in the C9. All these fragmentation patterns allowed to propose the co-elution of two positional isomers one with the epoxy and hydroxy groups in the same OA, bearing the epoxy group in C12, and the other with the epoxy group in a C10 position of other OA (Figure 5A).

The MS/MS spectrum of the ions that eluted at a major peak at 22.25 min (Figure 5B) showed an abundant product ion at *m/z* 603.533, formed by the loss of 312 Da (corresponding to the NL of OA+30 (16+14 Da) as RCOOH) plus NH_3, which means the NL of the oxidized OA, carrying both >O and OH groups. One more time, the minor product ion at *m/z* 493.387 allowed to pinpoint the positions of the OH and >O groups at the C9 and C12 of the oxidized OA, respectively.

The MS/MS spectrum of the ions that eluted at a major peak at 23.05 min (Figure 5C) showed abundant product ions at *m/z* 633.507 and *m/z* 603.533, formed due

399 to the NL of 282 Da and 312 Da, respectively, corresponding to the NL of the
400 non-modified OA as RCOOH and the NL of an OA carrying both OH and >O groups.
401 Due to the lack of minor product ions, positional isomers were difficult to identify for this
402 triolein derivative.
403

404 ## Discussion

405 Since oleic acid is the major component of several dietary oils, as olive and canola,
406 and being present mainly esterified to TAG, in this work, triolein was used as a frying oil
407 model to identify new primary oxidation TAGs that are formed when simulating the
408 common initial thermal process performed to heat the frying oils, thus preparing them to
409 fry different foods, such as chips, crisps, and snacks. For this, the C_{30} RP-LC-MS and
410 MS/MS were used for the first time to separate and identify the structural and functional
411 group isomers of thermally-oxidized TAGs of a frying oil simulant. The structural
412 identification was performed based on the exact mass measurements, RT, and diagnostic
413 fragment ions formed under MS/MS conditions. The RT of the oxidized triolein products
414 on the C_{30} column clearly changed with the modification type, and with the location of
415 the modifications along the fatty acyl chain (Figure S2). The multiple thermal-oxidation
416 products of triolein eluted at lower RT are due to the insertion of different oxygen
417 functional groups (from 1 oxygen to 4), thus increasing the polarity of the resultant
418 oxidized species. Therefore, with the progressive increase in the number of oxygen
419 groups, a decrease in the interactions of the oxidation products with the C_{30} column
420 occurred, resulting in lower RTs (Figure S2). This is in accordance with previous studies
421 performed with RP-LC of Fenton oxidized phospholipids.[31, 36]

422 Oleic acid is considered less prone to oxidation than polyunsaturated fatty acids
423 since it lacks bis-allylic carbons. However, due to the two allylic positions of the OA, one

carbon on each side of the double bond is more prone to oxidation. Its modifications can occur either in C8 or in C11 of the fatty acid acyl chain, or in the C9 or C10 in the event of a double bond delocalization.[37] In this work, multiple oxygenated derivatives (triolein + *n*O and triolein + *n*O - 2 Da, with *n* varying from 1 to 4) were identified for triolein submitted to 160 ºC for 5 min. Thus, these multiple oxidation products herein determined for triolein are related to the two allylic positions of the OA that can react with radical oxygen species formed during the thermal treatment. Epoxy and hydroperoxy derivatives of triolein,[38] and of large oligomeric triolein molecules (dimers, trimers, and tetramers),[39] have already been reported, when using thermal oxidation at 190 ºC for 6 hours. Furthermore, a large number of oxidation products of OA, as hydroxy, dihydroxy, hydroperoxy, and hydroxy-hydroperoxy derivatives, have already been reported but only upon highly oxidative Fenton reactions of phosphatidylcholine,[40] phosphatidylserine,[36] phosphatidylethanolamine,[41] or aminophospholipids.[31]

Beyond structural characterization, the separation of functional group isomers of short-thermally treated triolein was also evaluated. Herein, several hydroxy-, dihydroxy-, hydroperoxy-, dihydroperoxy-, hydroxy-hydroperoxy-, dihydroxy-hydroperoxy-, epoxy-, epoxy-hydroperoxy-, and epoxy-hydroxy-triolein derivatives were assessed (Table 1). From these, the separation of epoxy-, hydroperoxy-, and di-hydroperoxy-triolein derivatives was already attained when heating triolein in the dark for 3 weeks at 60 ºC.[25] Moreover, the functional isomers of different fats, as canola oil and margarine samples, have already been reported when using higher thermal oxidation temperature and time, where hydroperoxy and epoxy TAG derivatives were identified.[9, 28] However, at the conditions herein used (160 ºC, for 5 min) and using a less prone to oxidation TAG, it was possible to identify, for the first time in triolein or even in the oxidized OA of phospholipids upon Fenton conditions, the presence of dihydroxy-hydroperoxy,

epoxy-hydroxy, and epoxy-hydroperoxy derivatives. Although the fragmentation relative to the epoxy group (+ 14 Da) is in agreement with the fragmentation behavior described for epoxy-triolein derivatives,[25] it cannot be excluded the presence of a keto derivative,[36, 40] since the methodology used was not able to discriminate between epoxy and keto moieties. Besides, the formation of the detected epoxy-derivatives can result from the decomposition of hydroperoxyl radical intermediates, since the peroxyl radical might directly attack the double bond.[42] However, the approach herein used was not able to discriminate among this kind of triolein derivatives.

The present C_{30}-RP-LC-MS method also allowed the separation of positional isomers of triolein, a step beyond on the analysis of oxidized triolein achieved so far. Likewise, it was possible to identify different triolein oxidized derivatives, as the C9- and C10-hydroxy (Figure 1B), the C9- and C10-hydroperoxy (Figure 2A), and the C8, C9, and C10-epoxy (Figure 4B) triolein derivatives, whose positions were inferred by the interpretation of high-resolution MS/MS spectra. However, positional isomers with the same functional group but in different positions of the same fatty acyl chain are difficult to be separated in C_{30}-LC columns, and thus other locations of the functional groups cannot be excluded. Furthermore, separation of isomers with the same functional groups but distributed in different OA chains of the TAG was successfully achieved, as well as the separation of hydroxy, hydroperoxy, and epoxy derivatives.

The separation of isomers with the same molecular weight but with different combinations of hydroxy, hydroperoxy, and epoxy groups was also achieved, which included the modifications in the same OA chain or in different OAs (Table 1). It was possible to identify the (9-OH, 10-OH)-, (8-OH, 11-OH)-, and (9-OH, 12-OH)-triolein derivatives (Figure 1C, D), the (7-OOH, 10-OOH)-, (8-OOH, 10-OOH)-, (9-OOH, 10-OOH)-, and (9-OOH, 12-OOH)-triolein derivatives (Figure 2B, C), the

(9-OH, 10-OOH)- and (9-OH, 12-OOH)-triolein derivatives (Figure 3A, B), the (8-OH, 12-OH, 9-OOH)-triolein derivatives (Figure 3C), the (10>O, 9-OOH)- and (12>O, 9-OOH)-triolein derivative (Figure 4C, D), the (10>O, 9-OH)- and (12>O, 9-OH)-triolein derivative (Figure 5A, B). A similar result has never been achieved during the analysis of oxidized TAGs, revealing the capability of the C_{30} LC-MS methodology herein used to discriminate among different positional and structural isomers. Moreover, although this C_{30}-RP-LC-MS method has already been successfully applied for the separation of functional isomers of Fenton oxidized aminophospholipids, the separation of isomers with different group combinations was achieved for fatty acids more unsaturated than oleic acid.[31]

According to Figures 1-5, specific LC-MS/MS fragmentation patterns were identified for oxidized triolein. Fragments arising from the NL of water (18 Da) and H_2O_2 (34 Da) allowed to discriminate functional isomers, as hydroxy- and hydroperoxy-triolein derivatives, respectively. For this kind of molecules, the non-modified DAG (at *m/z* 603.533) originated the most abundant fragment ions in the MS/MS spectrum of modified products, bearing the oxidative modifications in only one OA chain. Fragment ions arising from the cleavage of the OA chain were also observed, allowing to pinpoint the position of the oxidative modifications across the OA backbone and to highlight the C9 (*m/z* 493.389) and C10 (*m/z* 477.394) to be the most prone positions to be modified. Moreover, the positions of the oxygenated moieties were assessed using the information from the positive-ion mode fragmentation between the oxygenated carbon and the carbon involved in the double bond in a vinylic position.[43, 44]

In the case of dihydroxy- and hydroperoxy-triolein derivatives, the NL of 18 Da or 34 Da were observed, respectively, while the combined NL of H_2O_2 and water (NL of 52 Da) was the characteristic of the MS/MS fragments in the hydroxy-

hydroperoxy-triolein derivatives. The dihydroperoxy-triolein derivatives bearing the two hydroperoxy moieties in different OA chains were discriminated due to the presence of highly abundant fragment ions arising from the NL of two H_2O_2 (2 x 34 Da, 68 Da). On the other side, the MS/MS spectra of dihydroxy-hydroperoxy-triolein derivatives, also bearing two modified OAs, showed a NL of 70 Da (NL of 2 x 18 Da plus 34 Da). The epoxy-triolein derivatives were discriminated due to the NL of 296 Da (NL of epoxy-OA (OA+14) as RCOOH) plus NH_3, but no specific fragmentation was assigned to the epoxy (>O) moiety. However, the presence of the abundant product ion, at *m/z* 599.501, attributed to the neutral loss of H_2O from the DAG bearing the epoxy-OA (formed after combined loss of non-modified OA plus NH_3), can suggest the appearance of two additional double bonds in the same OA chain, as already described for epoxy-TAGs.[42]

The epoxy-hydroperoxy-triolein derivatives bearing both >O and OOH groups in the same or in different OA chains were discriminated due to the NL of 328 Da (NL of epoxy-hydroperoxy-OA (OA+46) as RCOOH) or the NL of 314 Da (NL of hydroperoxy-OA) plus NH_3, respectively. Furthermore, the NL of 34 Da correspondent to the NL of the hydroperoxy group was also achieved. In addition, the epoxy-hydroxy-triolein derivatives were discriminated due to the characteristic NL of 18 Da from the NL of water due to the presence of the hydroxy group plus the NL of 312 Da (NL of epoxy-hydroxy-OA (OA+30) as RCOOH) plus NH_3.

In conclusion, this work showed that short-thermal treatment of triolein, such as that used to heat the frying oils preparing them to fry foods, induced lipids oxidation, promoting the formation of well-known epoxy and hydroperoxy TAGs, as well as a large range of primary oxidation products never reported, including dihydroxy-hydroperoxy and epoxy-hydroxy TAG derivatives. These conditions also promoted the formation of different positional isomers from lipid oxidation. All the thermally oxidized compounds

herein identified should be considered when evaluating the mechanisms of oxidation process of fried foods, as well as their flavor formation. Also, the knowledge gathered with this work can help to mitigate the lipid-derived reactive oxygen species that can occur during food frying. Overall, the presented method enables the identification of new classes of oxidized TAGs that may occur in common household frying conditions in food, thus giving new insights regarding the formation of oxidized TAGs under oil-thermal treatment.

Supporting Information/Associated Content

This material is available free of charge via the Internet at http://pubs.acs.org.

LC-MS spectra of the $[M+NH_4]^+$ ions of triolein before (A) and after 5 min of thermal oxidation (B), with the identification of the resultant long-chain oxidation products; Extracted ion current (XIC) chromatograms of the $[M+NH_4]^+$ ions of non-modified triolein (A), and its main long-chain oxidation products (B); LC-MS/MS spectra of the $[M+NH_4]^+$ ions of the non-modified triolein at *m/z* 902.818, that eluted at retention time 26.99 min; Schematic representation of the proposed fragmentation pathways of the positional isomers of the hydroxy derivative of triolein, at *m/z* 918.813, that eluted at retention time 24.23 min.

CRediT authorship contribution statement

Sílvia Petronilho*: Conceptualization, Supervision, Methodology, Formal analysis, Investigation, Visualization, Validation, Writing - original draft, Writing - review & editing. **Bruna Neves*:** Methodology, Formal analysis, Investigation,

Visualization, Writing - original draft. **Tânia Melo:** Methodology, Formal analysis, Investigation, Writing - review & editing. **Sara Oliveira:** Methodology, Formal analysis, Writing - review & editing. **Eliana Alves:** Investigation, Writing - review & editing. **Cristina Barros:** Methodology, Writing - review & editing. **Fernando Nunes:** Visualization, Writing - review & editing. **Manuel A. Coimbra:** Visualization, Writing - review & editing. **M. Rosário Domingues:** Conceptualization, Supervision, Formal analysis, Visualization, Resources, Validation, Writing - review & editing. *Equal contribution as first author.

Declaration of Competing Interest

The authors declare that they have no known competing financial interests or personal relationships that could have appeared to influence the work reported in this paper.

Acknowledgements

Thanks are due to the University of Aveiro and FCT/MCTES, QREN, COMPETE for the financial support to CESAM (UIDB/50017/2020 + UIDP/50017/2020) and LAQV-REQUIMTE (UIDB/50006/2020) research units, and CQ-VR at UTAD Vila Real (UIDP/00616/2020), and also to the Portuguese Mass Spectrometry Network (LISBOA-01-0145-FEDER-402-022125) through national funds, and when applicable, co-financed by FEDER, within the PT2020 Partnership Agreement and Compete 2020. Sílvia Petronilho thanks FCT for her Post-doc grant (SFRH/BPD/117213/2016). FCT is also thanked for the Scientific Employment Stimulus 2017, with a Junior Researcher contract to Eliana Alves (reference CEECIND/00971/2017). Tânia Melo thanks the research contract under the project Omics 4 Algae: Lipidomic tools for chemical phenotyping,

574 traceability and valorization of seaweeds from aquaculture as a sustainable source of high
575 added-value compounds (POCI-01-0145-FEDER-030962), funded by Centro2020,
576 through FEDER and PT2020.
577

References

1. Arslan, M.; Zou, X.; Shi, J.; Rakha, A.; Hu, X.; Zareef, M.; Zhai, X.; Basheer, S., Oil Uptake by Potato Chips or French Fries: A Review. *Eur. J. Lipid Sci. Tech.* **2018,** *120*, 1800058-800075. https://doi.org/10.1002/ejlt.201800058.

2. Song, J.; Kim, S.; Kim, J.; Kim, M.; Lee, S.; Jang, M.; Lee, J., Oxidative properties and moisture content in repeatedly used oils for French fries and breaded chickens during frying. *Eur. J. Lipid Sci. Tech.* **2017,** *119*, 1600279-1600286. https://doi.org/10.1002/ejlt.201600279.

3. Choe, E.; Min, D., Chemistry of deep-fat frying oils. *J. Food Sci.* **2007,** *72*, R77-R86. https://doi.org/10.1111/j.1750-3841.2007.00352.x.

4. Warner, K.; Neff, W.; Byrdwell, W.; Gardner, H., Effect of oleic and linoleic acids on the production of deep-fried odor in heated triolein and trilinolein. *J. Agr. Food Chem.* **2001,** *49*, 899-905. https://doi.org/10.1021/jf000822f.

5. Negroni, M.; D'Agostina, A.; Arnoldi, A., Effects of olive, canola, and sunflower oils on the formation of volatiles from the Maillard reaction of lysine with xylose and glucose. *J. Agr. Food Chem.* **2001,** *49*, 439-445. https://doi.org/10.1021/jf0003653.

6. Roldan, M.; Antequera, T.; Armenteros, M.; Ruiz, J., Effect of different temperature-time combinations on lipid and protein oxidation of sous-vide cooked lamb loins. *Food Chem.* **2014,** *149*, 129-136. https://doi.org/10.1016/j.foodchem.2013.10.079.

7. Li, X.; Li, J.; Wang, Y.; Cao, P.; Liu, Y., Effects of frying oils' fatty acids profile on the formation of polar lipids components and their retention in French fries over deep-frying process. *Food Chem.* **2017,** *237*, 98-105. https://doi.org/10.1016/j.foodchem.2017.05.100.

8. Cao, G.; Ruan, D.; Chen, Z.; Hong, Y.; Cai, Z., Recent developments and applications of mass spectrometry for the quality and safety assessment of cooking oil. *Trac-Trend. Anal. Chem.* **2017,** *96*, 201-211. https://doi.org/10.1016/j.trac.2017.07.015.

9. Kato, S.; Shimizu, N.; Hanzawa, Y.; Otoki, Y.; Ito, J.; Kimura, F.; Takekoshi, S.; Sakaino, M.; Sano, T.; Eitsuka, T.; Miyazawa, T.; Nakagawa, K., Determination of triacylglycerol oxidation

mechanisms in canola oil using liquid chromatography–tandem mass spectrometry. *Nature partner journals - Sci. Food* **2018,** *1*, 1-11. https://doi.org/doi:10.1038/s41538-017-0009-x.

10. Goicoechea, E.; Guillen, M., Analysis of Hydroperoxides, Aldehydes and Epoxides by H-1 Nuclear Magnetic Resonance in Sunflower Oil Oxidized at 70 and 100 ºC. *J. Agr. Food Chem.* **2010,** *58*, 6234-6245. https://doi.org/10.1021/jf1005337.

11. Barriuso, B.; Astiasaran, I.; Ansorena, D., A review of analytical methods measuring lipid oxidation status in foods: a challenging task. *Eur. Food Res. Technol.* **2013,** *236*, 1-15. https://doi.org/10.1007/s00217-012-1866-9.

12. Shahidi, F.; Zhong, Y., Lipid oxidation and improving the oxidative stability. *Chem. Soc. Rev.* **2010,** *39*, 4067-4079. https://doi.org/10.1039/b922183m.

13. Jurek, D.; Udilova, N.; Jozkowicz, A.; Nohl, H.; Marian, B.; Schulte-Hermann, R., Dietary lipid hydroperoxides induce expression of vascular endothelial growth factor (VEGF) in human colorectal tumor cells. *Faseb J.* **2004,** *18*, 97-99. https://doi.org/10.1096/fj.04-2111fje.

14. Yang, C.; Kendall, C.; Stamp, D.; Medline, A.; Archer, M.; Bruce, W., Thermally oxidized dietary fat and colon carcinogenesis in rodents. *Nutr. Cancer* **1998,** *30*, 69-73. https://doi.org/10.1080/01635589809514643.

15. Bou, R.; Codony, R.; Tres, A.; Decker, E.; Guardicila, F., Determination of hydroperoxides in foods and biological samples by the ferrous oxidation-xylenol orange method: A review of the factors that influence the method's performance. *Anal. Biochem.* **2008,** *377*, 1-15. https://doi.org/10.1016/j.ab.2008.02.029.

16. Nuchi, C.; Guardiola, F.; Bou, R.; Bondioli, P.; Della Bella, L.; Codony, R., Assessment of the Levels of Degradation in Fat Co-and Byproducts for Feed Uses and Their Relationships with Some Lipid Composition Parameters. *J. Agr. Food Chem.* **2009,** *57*, 1952-1959. https://doi.org/10.1021/jf803369h.

17. Martinez-Yusta, A.; Goicoechea, E.; Guillen, M., A Review of Thermo-Oxidative Degradation of Food Lipids Studied by H-1 NMR Spectroscopy: Influence of Degradative

Conditions and Food Lipid Nature. *Compr. Rev. Food Sci. F.* **2014,** *13*, 838-859. https://doi.org/10.1111/1541-665 4337.12090.

18. Xia, W.; Budge, S.; Lumsden, M., New H-1 NMR-Based Technique To Determine Epoxide Concentrations in Oxidized Oil. *J. Agr. Food Chem.* **2017,** *65*, 6717-6717. https://doi.org/10.1021/acs.jafc.7b03422.

19. Guillen, M.; Uriarte, P., Study by H-1 NMR spectroscopy of the evolution of extra Virgin olive oil composition submitted to frying temperature in an industrial fryer for a prolonged period of time. *Food Chem.* **2012,** *134*, 162-172. https://doi.org/10.1016/j.foodchem.2012.02.083.

20. Alexandri, E.; Ahmed, R.; Siddiqui, H.; Choudhary, M.; Tsiafoulis, C.; Gerothanassis, I., High Resolution NMR Spectroscopy as a Structural and Analytical Tool for Unsaturated Lipids in Solution. *Molecules* **2017,** *22, 1663-1735, https://doi.org/10.3390/molecules22101663*.

21. Zeb, A., Chemistry and liquid chromatography methods for the analyses of primary oxidation products of triacylglycerols. *Free Radical Res.* **2015,** *49*, 549-564. https://doi.org/10.3109/10715762.2015.1022540.

22. Xia, W.; Budge, S., Techniques for the Analysis of Minor Lipid Oxidation Products Derived from Triacylglycerols: Epoxides, Alcohols, and Ketones. *Compr. Rev. Food Sci. F.* **2017,** *16*, 735-756. https://doi.org/10.1111/1541-4337.12276.

23. Zeb, A.; Murkovic, M., Characterization of the effects of beta-carotene on the thermal oxidation of triacylglycerols using HPLC-ESI-MS. *Eur. J. Lipid Sci. Tech.* **2010,** *112*, 1218-1228. https://doi.org/10.1002/ejlt.201000392.

24. Zeb, A., Triacylglycerols composition, oxidation and oxidation compounds in camellia oil using liquid chromatography-mass spectrometry. *Chem. Phys. Lipids* **2012,** *165*, 608-614. https://doi.org/10.1016/j.chemphyslip.2012.03.004.

25. Neff, W.; Byrdwell, W., Characterization of model triacylglycerol (triolein, trilinolein and trilinolenin) autoxidation products via high-performance liquid chromatography coupled with

656 atmospheric pressure chemical ionization mass spectrometry. *J. Chromatogr. A* **1998,** *818*,
657 169-186. https://doi.org/10.1016/S0021-9673(98)00553-6.

658 26. Velasco, J.; Morales-Barroso, A.; Ruiz-Mendez, M.; Marquez-Ruiz, G., Quantitative
659 determination of major oxidation products in edible oils by direct NP-HPLC-DAD analysis.
660 *J. Chromatogr. A* **2018,** *1547*, 62-70. https://doi.org/10.1016/j.chroma.2018.03.014.

661 27. Lagarda, M.; Manez, J.; Manglano, P.; Farre, R., Lipid hydroperoxides determination in milk-
662 based infant formulae by gas chromatography. *Eur. J. Lipid Sci. Tech.* **2003,** *105*, 339-345.
663 https://doi.org/10.1002/ejlt.200390071.

664 28. Grüneis, V.; Fruehwirth, S.; Zehl, M.; Ortner, J. o.; Schamann, A.; König, J. r.; Pignitter, M.,
665 Simultaneous Analysis of Epoxidized and Hydroperoxidized Triacylglycerols in Canola Oil
666 and Margarine by LC-MS. *J. Agr. Food Chem.* **2019,** *67*, 10174-
667 10184. https://doi.org/10.1021/acs.jafc.9b03601.

668 29. Liu, Y.; Cong, P.; Li, B.; Song, Y.; Liu, Y.; Xu, J.; Xue, C., Effect of thermal processing
669 towards lipid oxidation and non-enzymatic browning reactions of Antarctic krill (*Euphausia*
670 *superba*) meal. *J. Sci. Food Agr.* **2018,** *98*, 5257-5268. https://doi.org/10.1002/jsfa.9064.

671 30. Criscuolo, A.; Zeller, M.; Cook, K.; Angelidou, G.; Fedorova, M., Rational selection of reverse
672 phase columns for high throughput LC-MS lipidomics. *Chem. Phys. Lipids* **2019,** *221*, 120-
673 127. https://doi.org/10.1016/j.chemphyslip.2019.03.006.

674 31. Colombo, S.; Criscuolo, A.; Zeller, M.; Fedorova, M.; Domingues, M.; Domingues, P.,
675 Analysis of oxidised and glycated aminophospholipids: Complete structural characterisation
676 by C30 liquid chromatography-high resolution tandem mass spectrometry. *Free Radical Bio.*
677 *Med.* **2019,** *144*, 144-155. https://doi.org/10.1016/j.freeradbiomed.2019.05.025.

678 32. Ni, Z.; Sousa, B.; Colombo, S.; Afonso, C.; Melo, T.; Pitt, A.; Spickett, C.; Domingues, P.;
679 Domingues, M.; Fedorova, M.; Criscuolo, A., Evaluation of air oxidized PAPC: A multi
680 laboratory study by LC-MS/MS. *Free Radical Bio. Med.* **2019,** *144*, 156-166.
681 https://doi.org/10.1016/j.freeradbiomed.2019.06.013.

33. Alves, E.; Melo, T.; Barros, M.; Domingues, M.; Domingues, P., Lipidomic Profiling of the Olive (*Olea europaea* L.) Fruit towards Its Valorisation as a Functional Food: In-Depth Identification of Triacylglycerols and Polar Lipids in Portuguese Olives. *Molecules* **2019,** *24*, 2555-2577. https://doi.org/10.3390/molecules24142555.

34. Wijesundera, C.; Ceccato, C.; Watkins, P.; Fagan, P.; Fraser, B.; Thienthong, N.; Perlmutter, P., Docosahexaenoic acid is more stable to oxidation when located at the sn-2 position of triacylglycerol compared to sn-1(3). *J. Am. Oil Chem. Soc.* **2008,** *85*, 543-548. https://doi.org/10.1007/s11746-008-1224-z.

35. Fazzari, M.; Khoo, N.; Woodcock, S.; Li, L.; Freeman, B.; Schopfer, F., Generation and esterification of electrophilic fatty acid nitroalkenes in triacylglycerides. *Free Radical Bio. Med.* **2015,** *87*, 113-124. https://doi.org/10.1016/j.freeradbiomed.2015.05.033.

36. Maciel, E.; Faria, R.; Santinha, D.; Domingues, M.; Domingues, P., Evaluation of oxidation and glyco-oxidation of 1-palmitoyl-2-arachidonoyl-phosphatidylserine by LC-MS/MS. *J. Chromatogr. B - Anal. Technol. Bio. Life Sci.* **2013,** *929*, 76-83. https://doi.org/10.1016/j.jchromb.2013.04.009.

37. Belitz, H. D.; Grosch, W.; Schieberle, P., Food Chemistry. 4th editon.; Springer-Verlag: Berlin, Heidelberg, **2009**.

38. Byrdwell, W.; Neff, W., Dual parallel electrospray ionization and atmospheric pressure chemical ionization mass spectrometry (MS), MS/MS and MS/MS/MS for the analysis of triacylglycerols and triacylglycerol oxidation products. *Rapid Commun. Mass Spectrom.* **2002,** *16*, 300-319. https://doi.org/10.1002/rcm.581.

39. Byrdwell, W.; Neff, W., Electrospray ionization MS of high MW TAG oligomers. *J. Am. Oil Chem. Soc.* **2004,** *81*, 13-26. https://doi.org/10.1007/s11746-004-0853-3.

40. Reis, A.; Domingues, P.; Ferrer-Correia, A.; Domingues, M., Tandem mass spectrometry of intact oxidation products of diacylphosphatidylcholines: evidence for the occurrence of the

oxidation of the phosphocholine head and differentiation of isomers. *J. Mass Spectrom.* **2004,** *39*, 1513-1522. https://doi.org/10.1002/jms.751.

41. Colombo, S.; Coliva, G.; Kraj, A.; Chervet, J.; Fedorova, M.; Domingues, P.; Domingues, M., Electrochemical oxidation of phosphatidylethanolamines studied by mass spectrometry. *J. Mass Spectrom.* **2018,** *53*, 223-233. https://doi.org/10.1002/jms.4056.

42. Giuffrida, F.; Destaillats, F.; Skibsted, L.; Dionisi, F., Structural analysis of hydroperoxy- and epoxy-triacylglycerols by liquid chromatography mass spectrometry. Chem. Phys. Lipids **2004**, *131*, 41-49. https://doi.org/10.1016/j.chemphyslip.2004.03.008.

43. Simoes, C.; Silva, A.; Domingues, P.; Laranjeira, P.; Paiva, A.; Domingues, M., Phosphatidylethanolamines Glycation, Oxidation, and Glycoxidation: Effects on Monocyte and Dendritic Cell Stimulation. *Cell Biochem. Biophys.* **2013,** *66*, 477-487. https://doi.org/10.1007/s12013-012-9495-2.

44. Domingues, M.; Simoes, C.; da Costa, J.; Reis, A.; Domingues, P., Identification of 1-palmitoyl-2-linoleoyl-phosphatidylethanolamine modifications under oxidative stress conditions by LC-MS/MS. *Biomed. Chromatogr.* **2009,** *23*, 588-601. https://doi.org/10.1002/bmc.1157.

723 **Table 1.** Oxidation products of triolein formed by short thermal-oxidation (160 ºC, 5 min)
724 identified by C_{30} RP-LC-MS as $[M+NH_4]^+$ adduct ions and confirmed by accurate mass
725 measurements and MS/MS data analysis.

Lipid species (C:N)	Calculated* *m/z*	Observed *m/z*	Error** (ppm)	Formula	RT (min)	TAG Modification
[MPoM][1]	766.6925	766.6915	-1.30	$C_{47}H_{92}NO_6$	23.86	-
[OOO] [2]	902.81766	902.8187	1.15	$C_{57}H_{108}NO_6$	26.99	-
[OOO+14Da]	916.79693	916.7969	-0.03	$C_{57}H_{106}NO_7$	23.46	Epoxy or Keto
					23.86	Epoxy or Keto
[OOO+16Da][3]	918.81258	918.8134	0.89	$C_{57}H_{108}NO_7$	23.26	Hydroxy
					24.23	Hydroxy
[OOO+30Da]	932.79184	932.7917	-0.15	$C_{57}H_{106}NO_8$	21.49	Epoxy-hydroxy
					22.25	Epoxy-hydroxy
					23.05	Epoxy-hydroxy
[OOO+32Da]	934.80749	934.8081	0.65	$C_{57}H_{108}NO_8$	22.35	Dihydroxy
					22.52	Dihydroxy
					23.12	Hydroperoxy
[OOO+46Da]	948.78676	948.7861	-0.69	$C_{57}H_{106}NO_9$	19.58	Epoxy-hydroperoxy
					22.65	Epoxy-hydroperoxy
[OOO+48Da]	950.80241	950.8012	-1.27	$C_{57}H_{108}NO_9$	20.86	Hydroxy-hydroperoxy
					22.45	Hydroxy-hydroperoxy
[OOO+64Da]	966.79732	966.7962	-1.16	$C_{57}H_{108}NO_{10}$	18.09	Dihydroxy-hydroperoxy
					19.07	Dihydroperoxy
					22.52	Dihydroperoxy

[1]MPoM (C14:0/C16:1/C14:0) – Internal standard, a triacylglyceride with 2 myristic and 1 palmitoleic acids.

[2]OOO (C18:1/C18:1/C18:1) – Triolein, a triacylglyceride with 3 oleic acids.

[3]Double bonds epoxidation cannot be excluded.

RT (min) – Retention time given in minutes.

Figure captions

Figure 1. LC-MS/MS spectra of the $[M+NH_4]^+$ ions of the hydroxy (A and B) and dihydroxy (C and D) derivatives of triolein at *m/z* 918.813 (RT 23.26 min and 24.23 min) and *m/z* 934.808 (RT 22.35 min and 22.52 min), respectively. The proposed structure and fragmentation pathways of the isomers of the hydroxy and dihydroxy derivatives of triolein are also shown. However, other possibilities of positional isomers of the hydroxy and dihydroxy derivatives of triolein cannot be excluded.

Figure 2. LC-MS/MS spectra of the $[M+NH_4]^+$ ions of the hydroperoxy (A) and dihydroperoxy (B and C) derivatives of triolein at *m/z* 934.808 (RT 23.12 min) and *m/z* 966.797 (RT 19.07 min and 22.52 min), respectively. The proposed structure and fragmentation pathways of the isomers of the hydroperoxy and di-hydroperoxy derivatives of triolein are also shown. However, other possibilities of positional isomers of the hydroperoxy and dihydroperoxy derivatives of triolein cannot be excluded.

Figure 3. LC-MS/MS spectra of the $[M+NH_4]^+$ ions of the hydroxy-hydroperoxy (A and B) and dihydroxy-hydroperoxy (C) derivatives of triolein at *m/z* 950.802 and *m/z* 966.699, respectively. The proposed structure and fragmentation pathways of the isomers of the hydroxy-hydroperoxy and dihydroxy-hydroperoxy derivatives of triolein are also shown. However, other possibilities of positional isomers of the hydroxy-hydroperoxy and dihydroxy-hydroperoxy derivatives of triolein cannot be excluded.

Figure 4. LC-MS/MS spectra of the $[M+NH_4]^+$ ions of the epoxy (A and B) and epoxy-hydroperoxy (C and D) derivatives of triolein at *m/z* 916.797 (RT 23.46 min and 23.86 min) and *m/z* 948.787 (RT 19.58 and 22.65 min), respectively. The proposed structure and fragmentation pathways of the isomers of the epoxy and epoxy-hydroperoxy derivatives of

752 triolein were also shown. However, other possibilities of positional isomers of the epoxy
753 and epoxy-hydroperoxy derivatives of triolein cannot be excluded, as well as the presence
754 of the keto derivative.
755
756 **Figure 5.** LC-MS/MS spectra of the $[M+NH_4]^+$ ions of the epoxy-hydroxy derivative of triolein
757 at *m/z* 932.792, that eluted at RT 21.49 (A), 22.25 (B), and 23.05 (C) min. The proposed structure
758 and fragmentation pathways of the isomers of the epoxy-hydroxy derivative of triolein were also
759 shown. However, other possibilities of positional isomers of the epoxy-hydroxy
760 derivatives of triolein cannot be excluded.

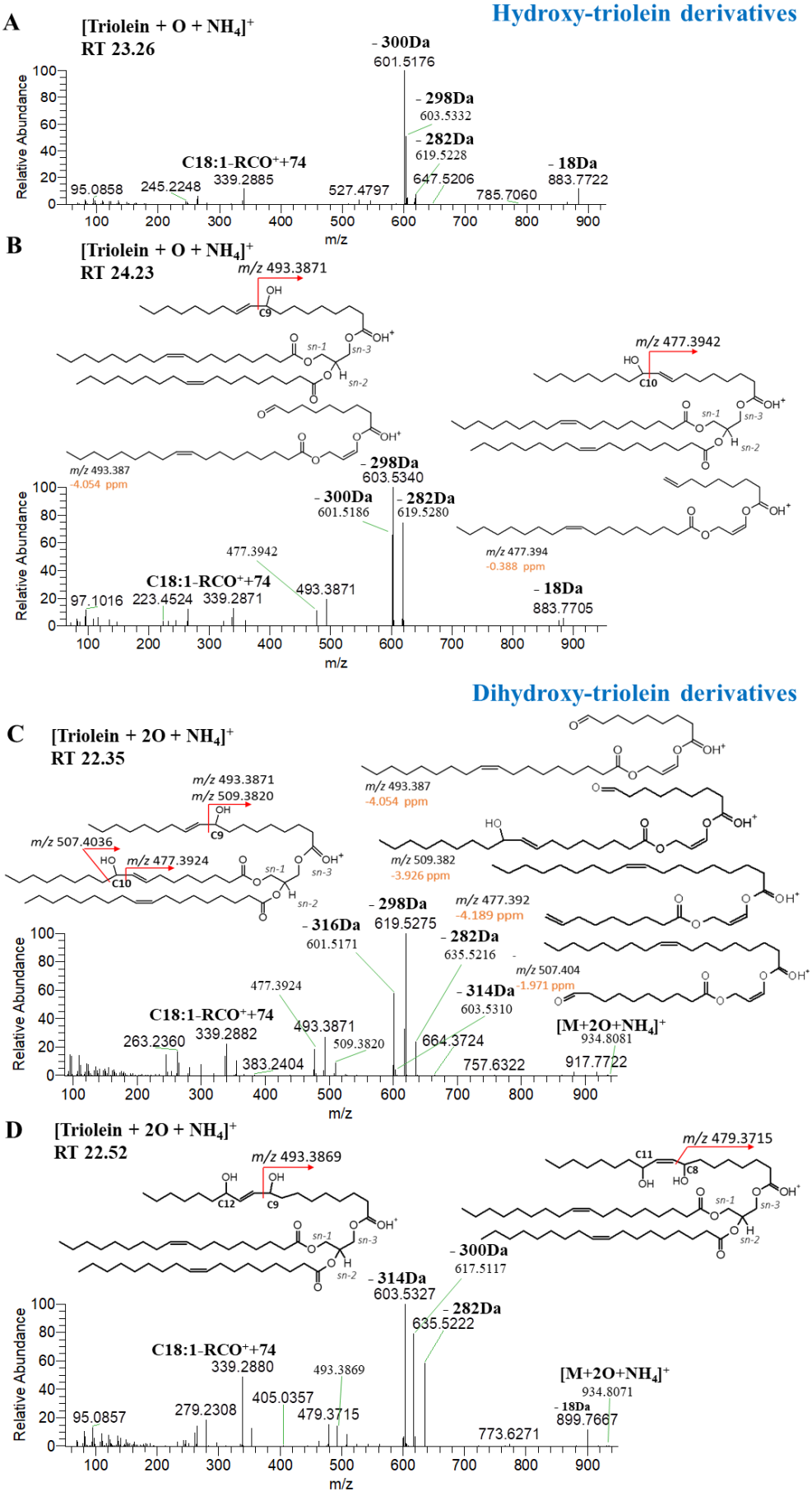
Hydroxy-triolein derivatives
A
[Triolein + O + NH4]+
RT 23.26
- 300Da
601.5176
- 298Da
603.5332
- 282Da
619.5228
- 18Da
883.7722
C18:1-RCO+ +74
339.2885
95.0858
245.2248
527.4797
647.5206
785.7060
Relative Abundance
m/z
B
[Triolein + O + NH4]+
RT 24.23
m/z 493.3871
m/z 477.3942
m/z 493.387
-4.054 ppm
- 298Da
603.5340
- 300Da
601.5186
- 282Da
619.5280
m/z 477.394
-0.388 ppm
477.3942
C18:1-RCO+ +74
493.3871
- 18Da
883.7705
97.1016
223.4524
339.2871
Dihydroxy-triolein derivatives
C
[Triolein + 2O + NH4]+
RT 22.35
m/z 493.3871
m/z 509.3820
m/z 507.4036
m/z 477.3924
m/z 493.387
-4.054 ppm
m/z 509.382
-3.926 ppm
- 298Da
619.5275
m/z 477.392
-4.189 ppm
- 316Da
601.5171
- 282Da
635.5216
m/z 507.404
-1.971 ppm
- 314Da
603.5310
477.3924
C18:1-RCO+ +74
339.2882
493.3871
509.3820
[M+2O+NH4]+
934.8081
263.2360
383.2404
664.3724
757.6322
917.7722
D
[Triolein + 2O + NH4]+
RT 22.52
m/z 493.3869
m/z 479.3715
- 300Da
617.5117
- 314Da
603.5327
- 282Da
635.5222
C18:1-RCO+ +74
339.2880
493.3869
[M+2O+NH4]+
934.8071
- 18Da
899.7667
95.0857
279.2308
405.0357
479.3715
773.6271

Figure 1.

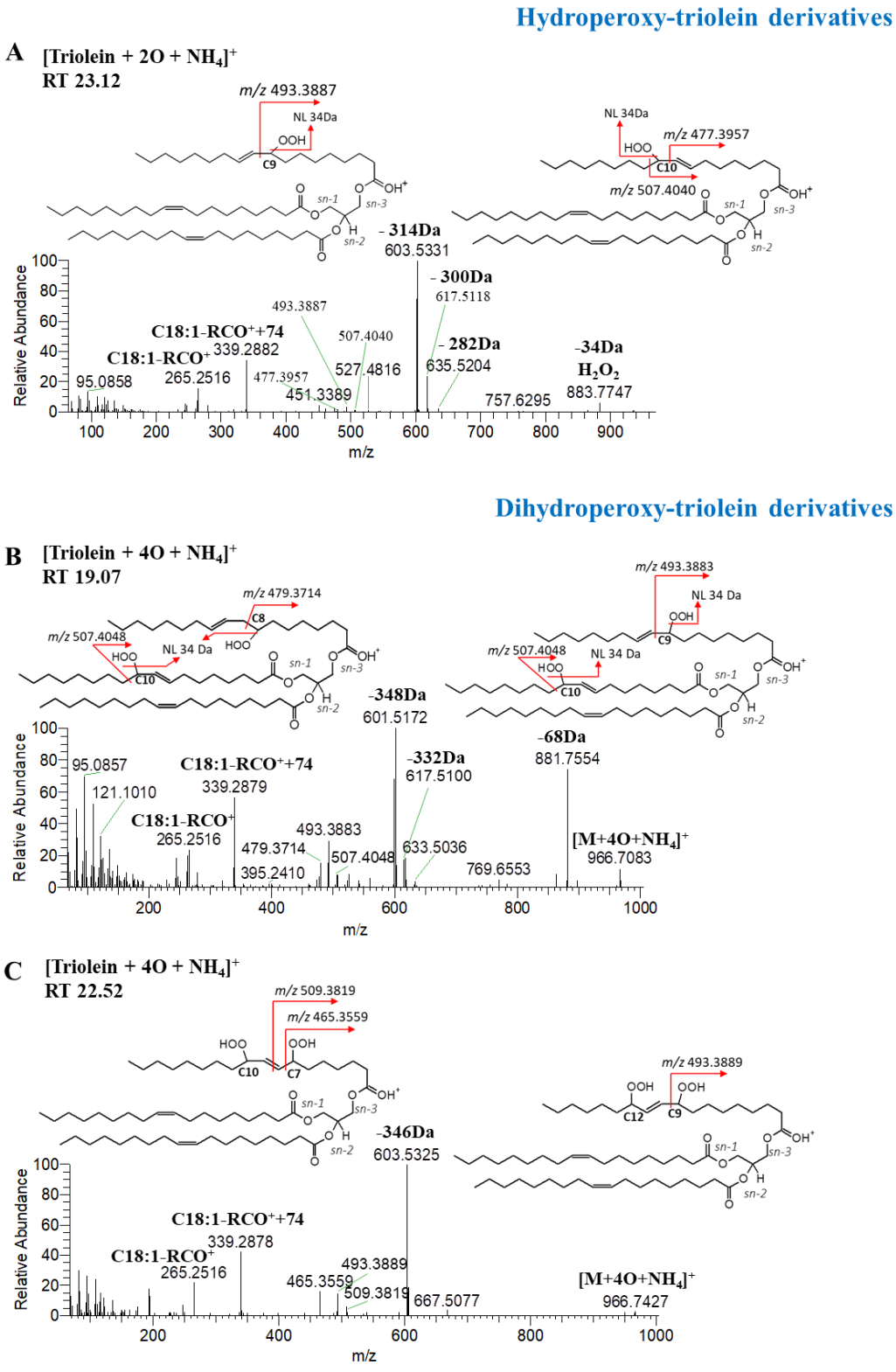
Hydroperoxy-triolein derivatives
A
[Triolein + 2O + NH4]+
RT 23.12
m/z 493.3887
NL 34Da
OOH
C9
m/z 477.3957
NL 34Da
HOO
C10
m/z 507.4040
sn-1
sn-2
sn-3
-314Da
603.5331
-300Da
617.5118
493.3887
C18:1-RCO+74
339.2882
C18:1-RCO+
265.2516
507.4040
-282Da
635.5204
527.4816
477.3957
451.3389
95.0858
757.6295
-34Da
H2O2
883.7747
Relative Abundance
m/z
Dihydroperoxy-triolein derivatives
B
[Triolein + 4O + NH4]+
RT 19.07
m/z 479.3714
C8
m/z 507.4048
HOO
NL 34 Da
HOO
C10
m/z 493.3883
NL 34 Da
OOH
C9
m/z 507.4048
NL 34 Da
HOO
C10
-348Da
601.5172
-68Da
881.7554
95.0857
121.1010
C18:1-RCO+74
339.2879
C18:1-RCO+
265.2516
-332Da
617.5100
493.3883
479.3714
507.4048
633.5036
395.2410
769.6553
[M+4O+NH4]+
966.7083
Relative Abundance
m/z
C
[Triolein + 4O + NH4]+
RT 22.52
m/z 509.3819
m/z 465.3559
HOO
OOH
C10
C7
m/z 493.3889
OOH
OOH
C12
C9
-346Da
603.5325
C18:1-RCO+74
339.2878
C18:1-RCO+
265.2516
493.3889
465.3559
509.3819
667.5077
[M+4O+NH4]+
966.7427
Relative Abundance
m/z

Figure 2.

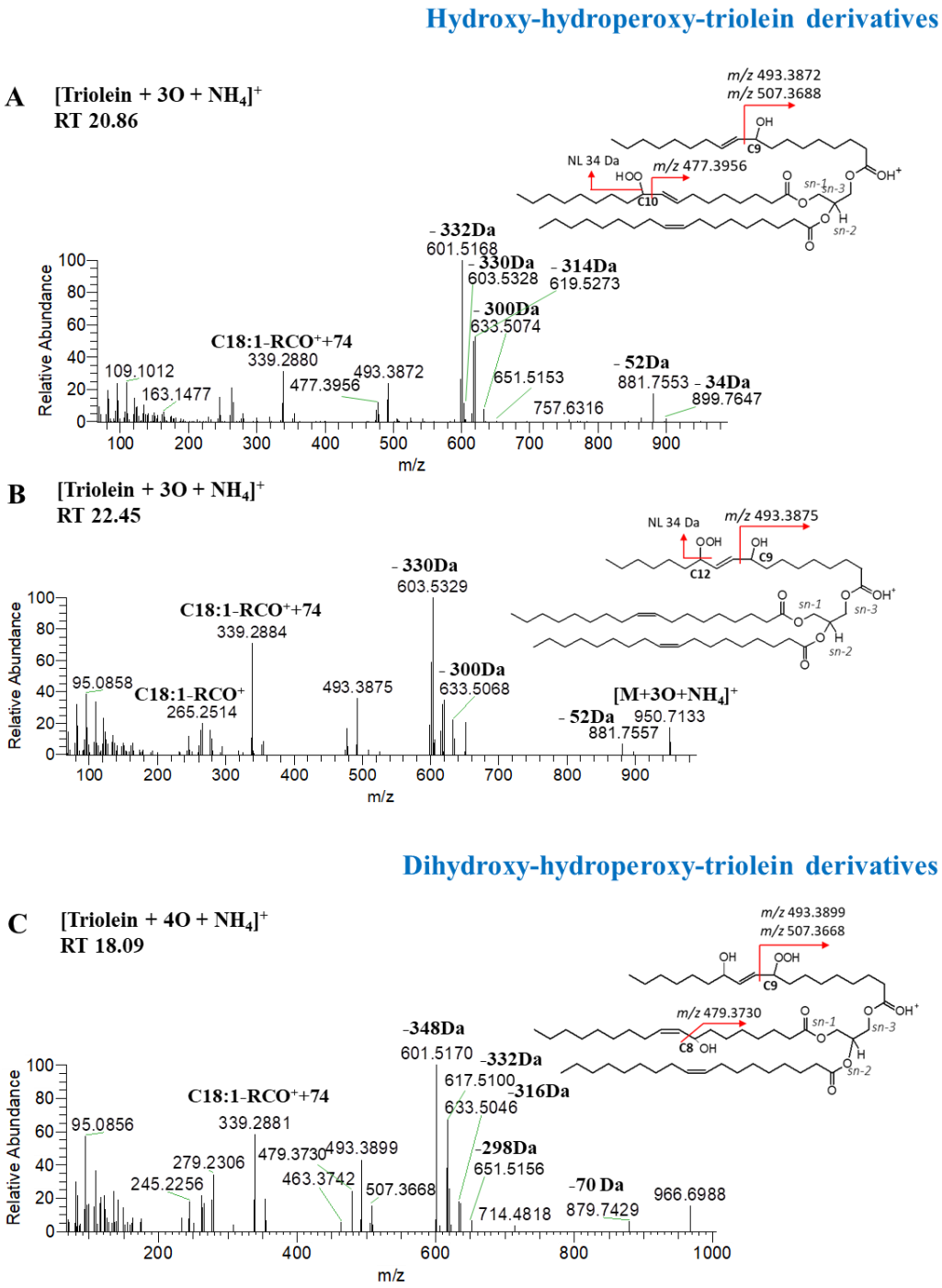
Hydroxy-hydroperoxy-triolein derivatives
A
[Triolein + 3O + NH4]+
RT 20.86
m/z 493.3872
m/z 507.3688
NL 34 Da
m/z 477.3956
- 332Da
601.5168
- 330Da
603.5328
- 314Da
619.5273
- 300Da
633.5074
C18:1-RCO+ +74
339.2880
109.1012
163.1477
477.3956
493.3872
651.5153
- 52Da
881.7553
- 34Da
899.7647
757.6316
Relative Abundance
m/z
B
[Triolein + 3O + NH4]+
RT 22.45
NL 34 Da
m/z 493.3875
- 330Da
603.5329
C18:1-RCO+ +74
339.2884
- 300Da
633.5068
95.0858
C18:1-RCO+
265.2514
493.3875
[M+3O+NH4]+
- 52Da
881.7557
950.7133
Relative Abundance
m/z
Dihydroxy-hydroperoxy-triolein derivatives
C
[Triolein + 4O + NH4]+
RT 18.09
m/z 493.3899
m/z 507.3668
m/z 479.3730
-348Da
601.5170
-332Da
617.5100
-316Da
633.5046
-298Da
651.5156
C18:1-RCO+ +74
339.2881
95.0856
279.2306
245.2256
479.3730
493.3899
463.3742
507.3668
-70 Da
879.7429
714.4818
966.6988
Relative Abundance
m/z

Figure 3.

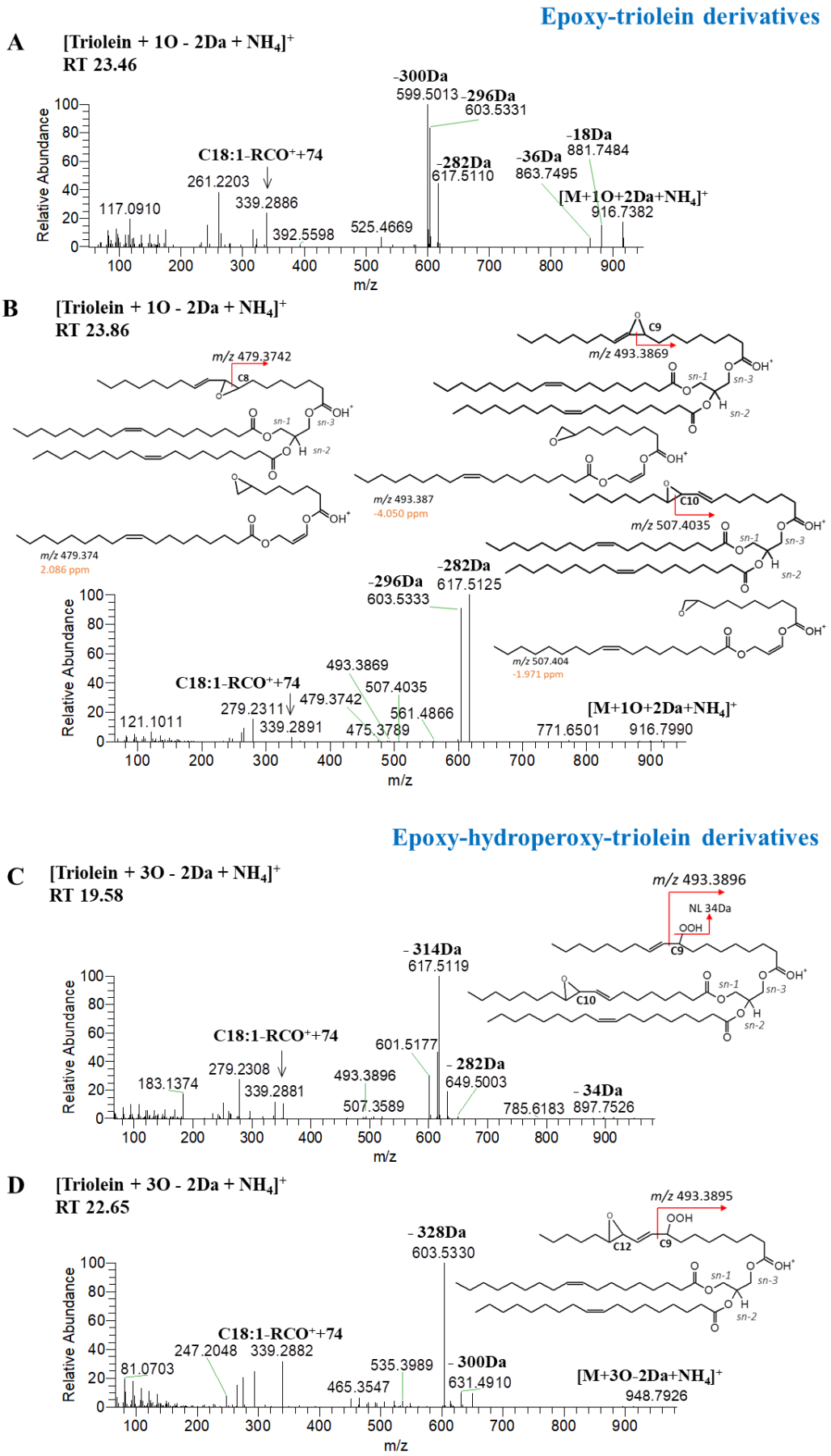
Epoxy-triolein derivatives
A
[Triolein + 1O - 2Da + NH4]+
RT 23.46
-300Da
599.5013
-296Da
603.5331
-18Da
881.7484
-36Da
863.7495
-282Da
617.5110
C18:1-RCO+ +74
261.2203
339.2886
117.0910
392.5598
525.4669
[M+1O+2Da+NH4]+
916.7382
Relative Abundance
m/z
B
[Triolein + 1O - 2Da + NH4]+
RT 23.86
m/z 479.3742
C8
m/z 479.374
2.086 ppm
m/z 493.3869
C9
m/z 493.387
-4.050 ppm
m/z 507.4035
C10
m/z 507.404
-1.971 ppm
-282Da
617.5125
-296Da
603.5333
C18:1-RCO+ +74
279.2311
339.2891
121.1011
493.3869
479.3742
507.4035
561.4866
475.3789
[M+1O+2Da+NH4]+
771.6501
916.7990
Epoxy-hydroperoxy-triolein derivatives
C
[Triolein + 3O - 2Da + NH4]+
RT 19.58
m/z 493.3896
NL 34Da
OOH
C9
C10
-314Da
617.5119
C18:1-RCO+ +74
279.2308
339.2881
183.1374
601.5177
493.3896
507.3589
-282Da
649.5003
-34Da
785.6183
897.7526
D
[Triolein + 3O - 2Da + NH4]+
RT 22.65
m/z 493.3895
OOH
C12
C9
-328Da
603.5330
C18:1-RCO+ +74
247.2048
339.2882
81.0703
535.3989
465.3547
-300Da
631.4910
[M+3O-2Da+NH4]+
948.7926

Figure 4.

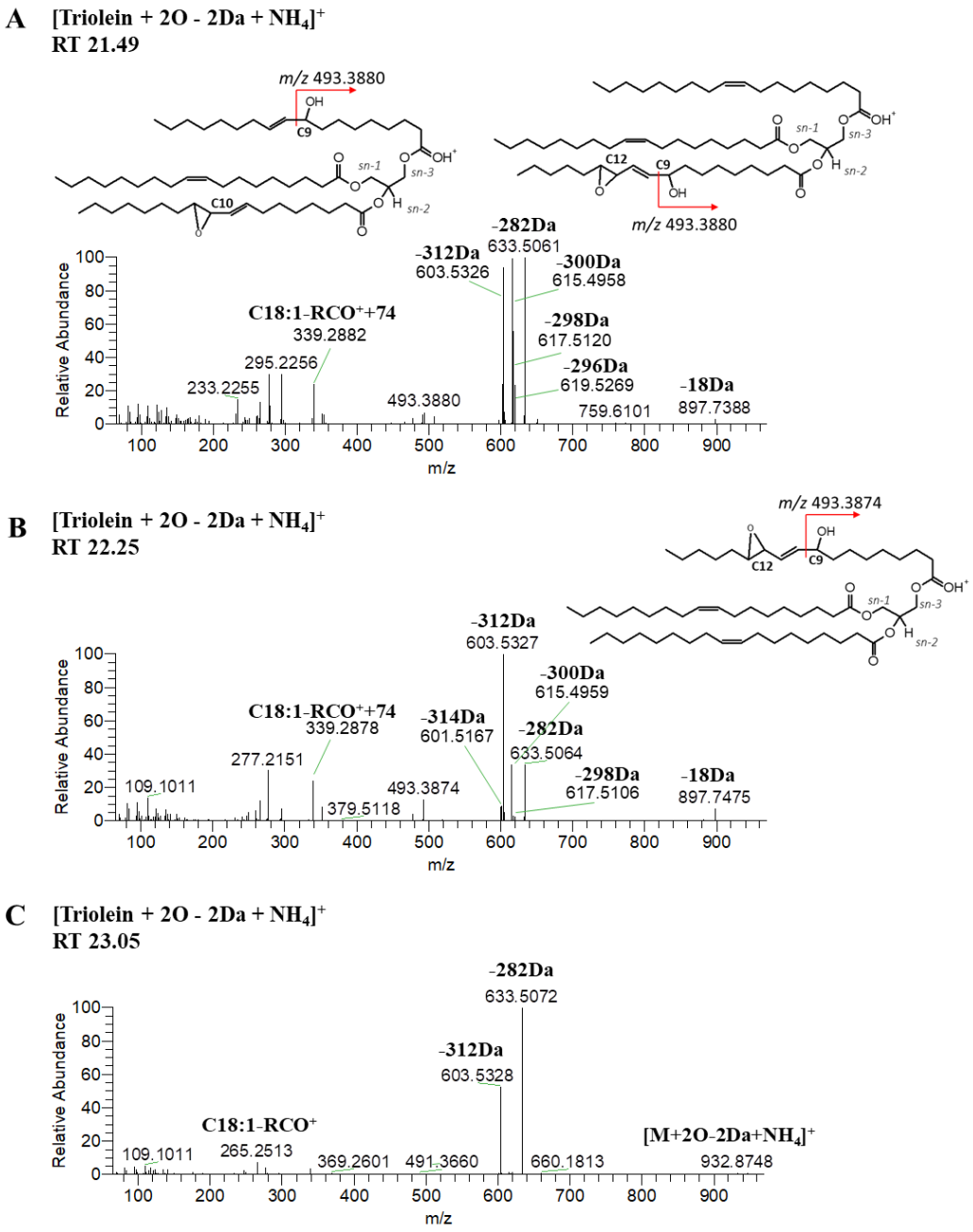
A
[Triolein + 2O - 2Da + NH4]+
RT 21.49
m/z 493.3880
OH
C9
C10
sn-1
sn-3
sn-2
OH+
C12
C9
OH
m/z 493.3880
-282Da
633.5061
-312Da
603.5326
-300Da
615.4958
C18:1-RCO+-74
339.2882
-298Da
617.5120
295.2256
-296Da
619.5269
233.2255
493.3880
-18Da
759.6101
897.7388
Relative Abundance
m/z
B
[Triolein + 2O - 2Da + NH4]+
RT 22.25
m/z 493.3874
C12
C9
OH
-312Da
603.5327
-300Da
615.4959
C18:1-RCO+-74
339.2878
-314Da
601.5167
-282Da
633.5064
277.2151
-298Da
617.5106
-18Da
109.1011
493.3874
379.5118
897.7475
Relative Abundance
m/z
C
[Triolein + 2O - 2Da + NH4]+
RT 23.05
-282Da
633.5072
-312Da
603.5328
C18:1-RCO+
265.2513
[M+2O-2Da+NH4]+
109.1011
369.2601
491.3660
660.1813
932.8748
Relative Abundance
m/z

Figure 5.

***TOC graphic**

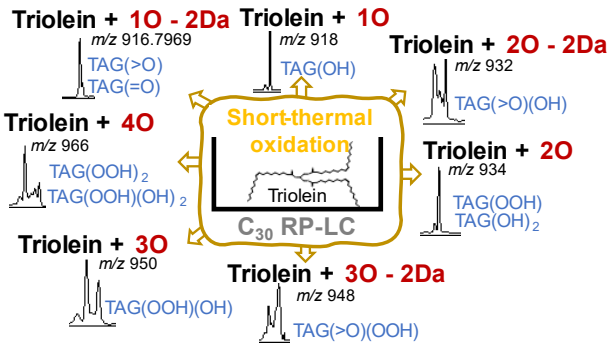
Triolein + 1O - 2Da
m/z 916.7969
TAG(>O)
TAG(=O)
Triolein + 1O
m/z 918
TAG(OH)
Triolein + 2O - 2Da
m/z 932
TAG(>O)(OH)
Triolein + 4O
m/z 966
TAG(OOH)2
TAG(OOH)(OH)2
Short-thermal oxidation
Triolein
C30 RP-LC
Triolein + 2O
m/z 934
TAG(OOH)
TAG(OH)2
Triolein + 3O
m/z 950
TAG(OOH)(OH)
Triolein + 3O - 2Da
m/z 948
TAG(>O)(OOH)

* Supplementary Figures

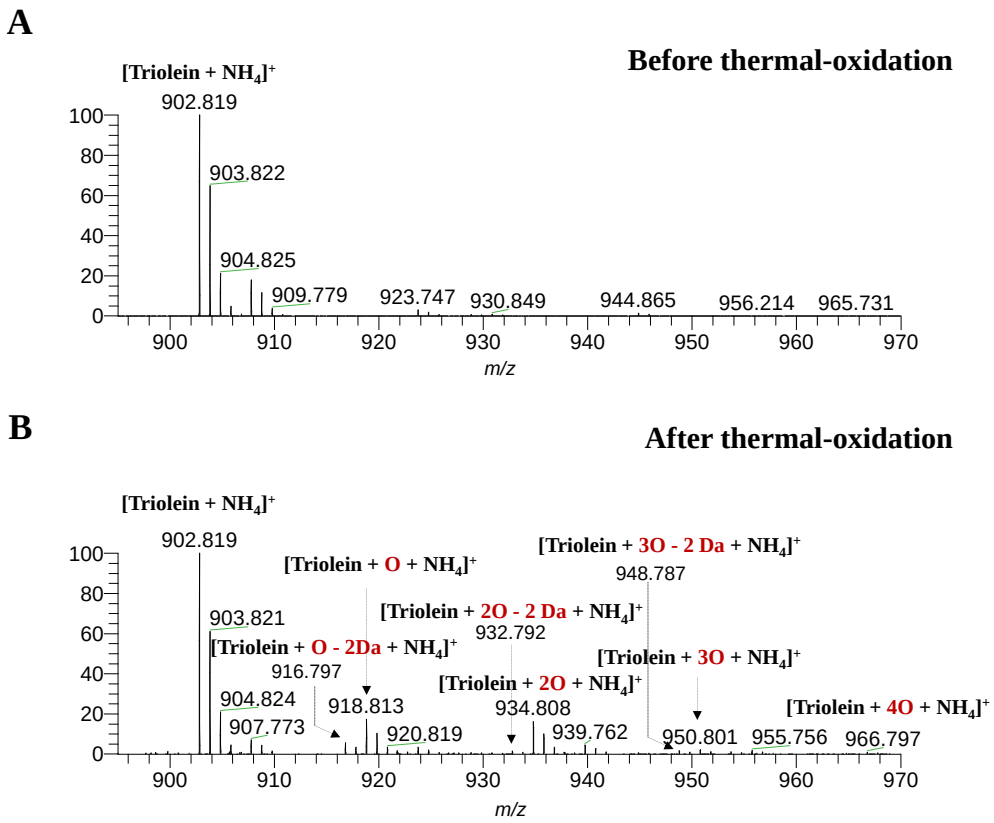

Figure S1. LC-MS spectra of the $[M+NH_4]^+$ ions of triolein before (A) and after 5 min of thermal-oxidation (B), with the identification of the resultant long-chain oxidation products.

A **Before thermal-oxidation**

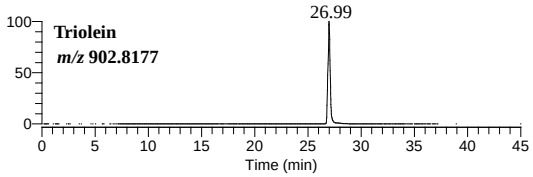

B **After thermal-oxidation**

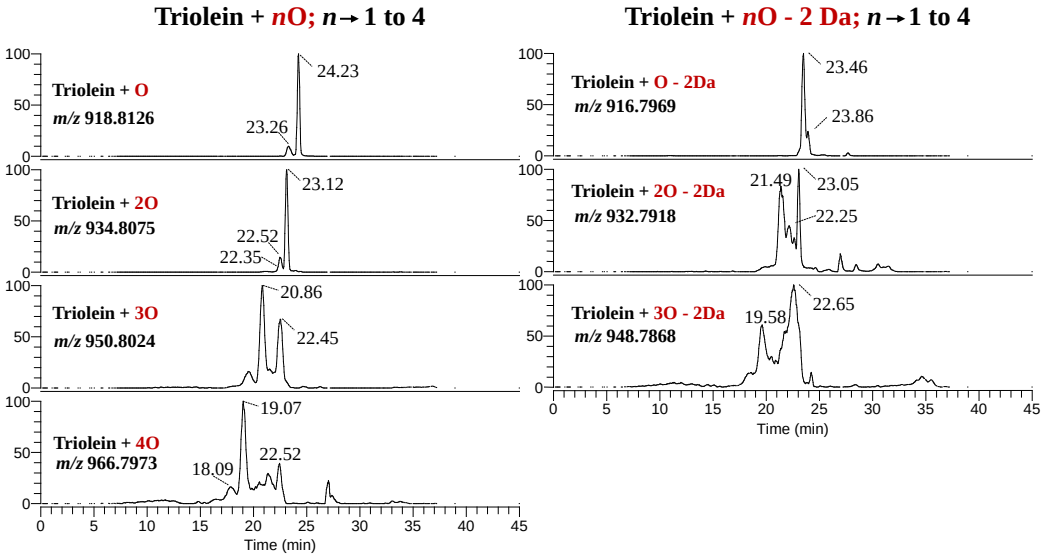

Figure S2. Extracted ion current (XIC) chromatograms of the $[M+NH_4]^+$ ions of non-modified triolein (A), and its main long-chain oxidation products (B).

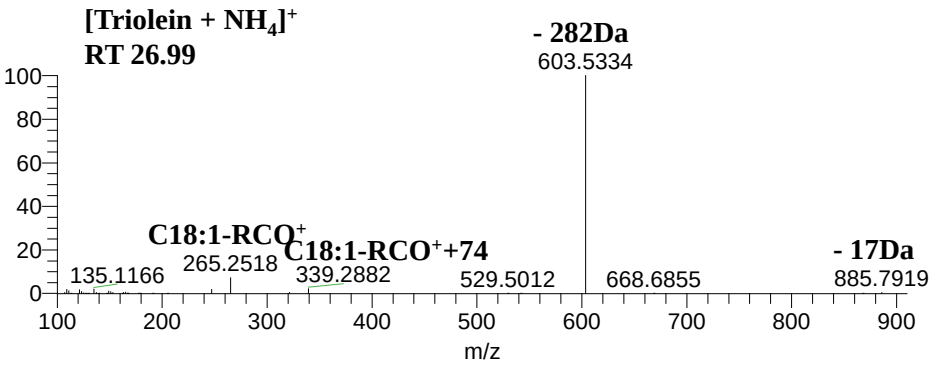

Figure S3. LC-MS/MS spectra of the $[M+NH_4]^+$ ions of the non-modified triolein at *m/z* 902.818, that eluted at retention time 26.99 min.

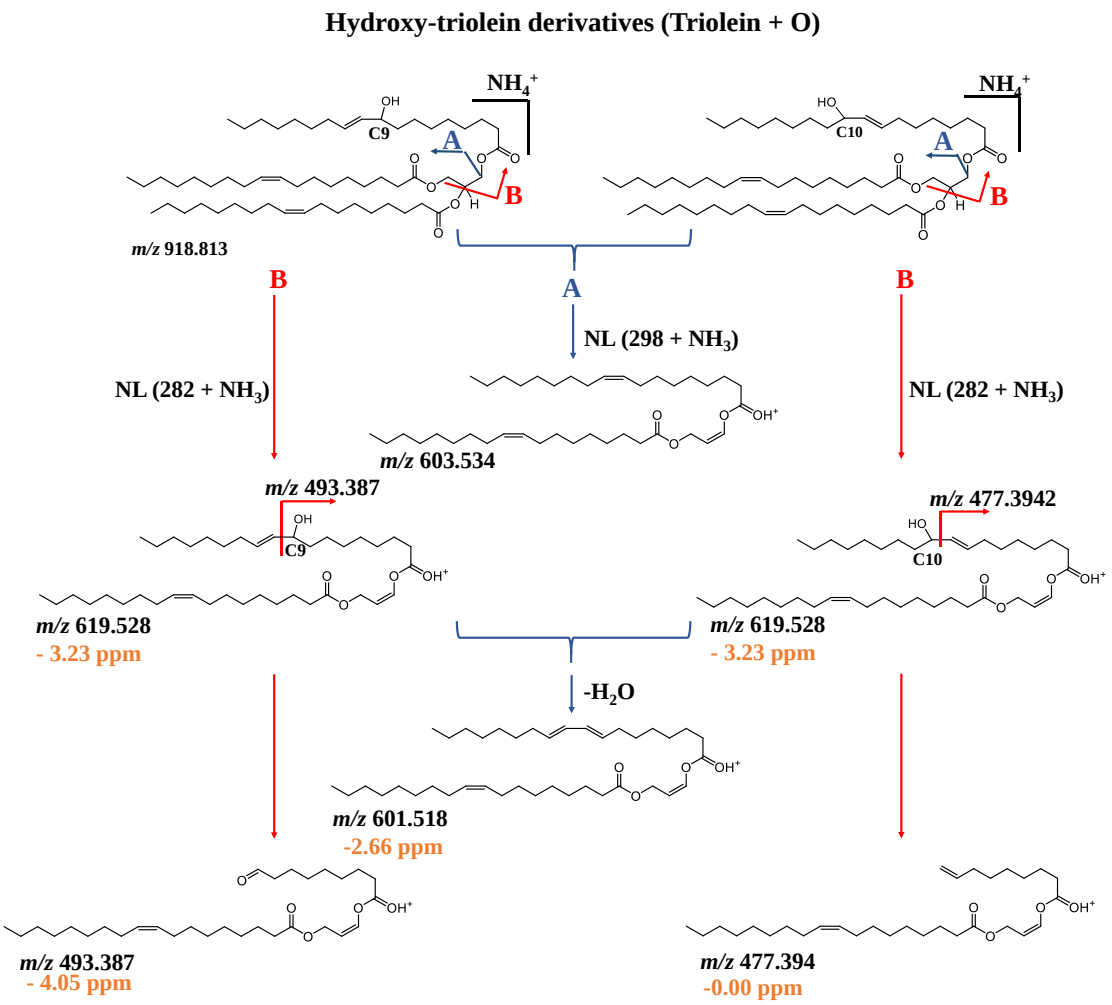

Figure S4. Schematic representation of the proposed fragmentation pathways of the positional isomers of the hydroxy derivative of triolein, at *m/z* 918.813, that eluted at retention time 24.23 min.